

Cite this: *RSC Med. Chem.*, 2025, 16, 1715

# Biocompatible glycolipid derived from bhilawanol as an antibiofilm agent and a promising platform for drug delivery†

Tohira Banoo,<sup>a</sup> Abhijit Ghosh,<sup>b</sup> Priyasha Mishra, <sup>b</sup>  
Sanhita Roy<sup>b</sup> and Subbiah Nagarajan <sup>\*a</sup>

Stimuli-responsive smart materials for biomedical applications have gained significant attention because of their potential for selectivity and sensitivity in biological systems. Even though ample stimuli-responsive materials are available, the use of traditional Ayurvedic compounds in the fabrication of pharmaceuticals is limited. Among various materials, gels are one of the essential classes because of their molecular-level tunability with little effort from the environment. In this study, we report a simple synthesis method for multifunctional glycolipids using a starting material derived from biologically significant natural molecules and carbohydrates in good yields. The synthesized glycolipids were prone to form a hydrogel by creating a 3D fibrous architecture. The mechanism of bottom-up assembly involving the molecular-level interaction was studied in detail using SEM, XRD, FTIR, and NMR spectroscopy. The stability, processability, and thixotropic behavior of the hydrogel were investigated through rheological measurements, and it was identified to be more suitable for biomedical applications. To evaluate the potential application of the self-assembled hydrogel in the field of medicine, we encapsulated a natural drug, curcumin, into a gel and studied its pH as a stimuli-responsive release profile. Interestingly, the encapsulated drug was released both in acidic and basic pH levels at a different rate, as identified using UV-vis spectroscopy. It is worth mentioning that the gelator used for fabricating smart soft materials displays significant potential in selectively compacting the biofilm formed by *Streptococcus pneumoniae*. We believe that the reported multifunctional hydrogel derived from bhilawanol-based glycolipid holds great promise in medicine.

Received 23rd October 2024,  
Accepted 19th January 2025

DOI: 10.1039/d4md00828f

rsc.li/medchem

## Introduction

In recent years, significant progress and technological advancement have been achieved in developing drug delivery systems that aim to enhance the therapeutic effect with higher efficiency and target drug delivery.<sup>1</sup> Conventional drug delivery systems, however, follow a non-specific distribution path in living systems and pose adverse side effects, including toxicity in healthy tissues and development of multi-drug resistance.<sup>2</sup> To overcome these limitations and decrease the exposure of healthy organs and cells to the drug dose, an advanced and smart stimuli-responsive drug delivery system (DDS) has been developed to achieve a controlled and

targeted delivery profile. The smart DDS does not release the drug before reaching the specific targeted organ or cell and only releases it in a specific manner in response to external stimuli.<sup>3,4</sup> Thus, smart DDS are considered fascinating interventions for various diseases owing to their lower drug concentrations, minimum drug toxicity, and better therapeutic efficiency.<sup>5</sup> In this work, we synthesized a low molecular weight gelator-based pH stimuli-responsive drug delivery system from carbohydrates and a molecule represented in a traditional system of medicines. pH trigger is one of the important stimuli among the different stimuli-responsive DDSs, as in living systems, different parts have different pH values, which provides a great scope for pH-stimulated drug delivery systems. Carbohydrates are versatile compounds displaying a broad range of applications in food, pharmaceuticals, cosmetics, and other sectors owing to their non-toxic, biodegradable, and biocompatible properties. The growing interest in carbohydrate research stems from their critical role in biological systems, such as glycoproteins found in the extracellular matrix, which are involved in signalling pathways, cell-cell interactions, and cell-matrix interactions. By considering the increasing demand for glycoconjugates in

<sup>a</sup> Assembled Organic and Hybrid Material Lab, Department of Chemistry, National Institute of Technology Warangal, Hanumakonda-506004, Telangana, India.

E-mail: snagarajan@nitw.ac.in, snrajannpt@yahoo.co.in

<sup>b</sup> Dr. Chigurupati Nageswara Rao Ocular Pharmacology Research Centre, LV Prasad Eye Institute, Hyderabad – 500034, Telangana, India

† Electronic supplementary information (ESI) available: NMR spectra, mass spectra, biological investigation details. See DOI: <https://doi.org/10.1039/d4md00828f>



biological applications, this study focuses on gluconamide-based amphiphiles derived from renewable resources such as  $\delta$ -gluconolactone and bhilawanol. In particular, glycoconjugates are one of the most essential drug delivery systems (DDSs) utilized for many years, and they have gained significant importance over time.<sup>6–8</sup> It is worth mentioning that gluconamide-based amphiphiles used for the construction of stimuli-responsive drug delivery systems have been evaluated for their cytotoxic behaviour as well. We further explored the antibacterial properties by considering most health issues caused by different bacteria, ranging from minor health risks to major ones in animals and plants.<sup>9</sup>

The formation of valuable chemical commodities using renewable resources is a topic of great interest.<sup>10</sup> Our research aims to develop building blocks from natural resources to generate soft nanomaterials such as hydrogels, organogels, and surfactants.<sup>11</sup> In the present investigation, we generated a series of amphiphiles from biologically relevant molecules such as bhilawanol and glucono- $\delta$ -lactone. Bhilawanol is a natural phenolic compound found in *Semecarpus anacardium*, a plant well-known for its antimicrobial, antidiabetic, and anti-arthritis properties in the Ayurvedic and Siddha systems of medicine.<sup>12–14</sup> Glucono- $\delta$ -lactone is one of the important naturally occurring carbohydrates, widely used in food additives as a sequestrant, acidifier, or a curing, pickling, or leavening agent.<sup>15–17</sup> In addition, carbohydrates are widely used for biological applications owing to their superior properties such as biodegradability, nontoxicity, renewability, and abundant availability.<sup>18,19</sup> The judicious conjugation of glucono- $\delta$ -lactone with bhilawanol furnished a bio-based building block, which, upon molecular self-assembly utilizing various intermolecular interactions, generated a hydrogel.<sup>20,21</sup> It is worth mentioning that molecular self-assembly is a powerful tool to develop highly functional and molecularly defined materials. Among the various assembled materials, hydrogels are one of the important types and possess a wide range of applications in pharmaceuticals and medicine, including medical implants, drug delivery systems, drug formulations, and tissue engineering.<sup>22</sup> To date, the synthesis of glycolipid from bhilawanol, otherwise called urushiol, is not known in the literature. Nevertheless, the design strategy is based on the significance of glycolipid derived from cardanol.<sup>23</sup> Unlike polymers, small amphiphilic molecules self-assemble simultaneously into a complex structure without the involvement of any external energy.<sup>24</sup> The forces that direct the molecular self-assembly are weak noncovalent interactions such as hydrogen bonds, van der Waals forces, and  $\pi$ - $\pi$  stacking.<sup>25</sup> These forces are tunable by external stimuli such as temperature, pressure, pH, receptors, and interactive and instructive species.<sup>26</sup> Several research reports have documented the fabrication of gels from carbohydrates, displaying promising applications in tissue engineering, biomedical applications, semiconductor devices, sensors, etc.<sup>27,28</sup> However, in this report, we developed a simple strategy for the synthesis of glycolipid by conjugation of

bhilawanol with glucono- $\delta$ -lactone in good yield. The bottom-up assembly of bhilawanol glycolipid in various solvents led to gel formation, utilizing intermolecular interactions such as H-bonding,  $\pi$ - $\pi$  interaction, and van der Waals forces. Interestingly, the biologically significant supramolecular hydrogel derived from bhilawanol glycolipid encapsulated a natural drug, curcumin, and displayed pH-responsive release profile. Antibacterial and cytotoxicity studies revealed the promise of using bhilawanol glycolipid in the field of drug delivery and biology.

## Experimental section

### Materials and general methods

All the required chemicals and solvents used for the synthesis of bhilawanol glycolipids were purchased from Sigma-Aldrich, TCI Chemicals, Alfa Aesar, Avra, SRL, and Spectrochem, and were used as such without further purification. Bhilawanol was extracted from *Semecarpus anacardium* seeds. LR-grade solvents were purchased and used for column chromatography and the required purification processes of the compounds. AR-grade solvents were used for gelation studies. The pre-coated Merck silica gel plates were used to monitor the reaction progress by thin-layer chromatography (TLC) and the spots were visualized using any one or a combination of the following visualizing agents such as UV detection,  $\text{KMnO}_4$ , *p*-anisaldehyde,  $\text{H}_2\text{SO}_4$  spray, or molecular iodine.

$^1\text{H}$  and  $^{13}\text{C}$  NMR spectra for bhilawanol glycolipids and all other starting materials were recorded on a Bruker Avance 400 MHz instrument in either  $\text{CDCl}_3$  or  $\text{CDCl}_3$  with a few drops of  $\text{DMSO-d}_6$  or  $\text{DMSO-d}_6$  at room temperature. TMS was used as an internal standard; chemical shifts ( $\delta$ ) are reported in parts per million (ppm) with respect to the internal standard. TMS and coupling constants (*J*) are given in Hz. Proton multiplicity is assigned using the following abbreviations: singlet (s), doublet (d), triplet (t), quartet (q), and multiplet (m). Electrospray ionization mass spectra (ESI-MS) were recorded in the positive mode with a Thermo Fisher LCQ Advantage Max. Instrument by dissolving the solid sample in acetonitrile or methanol.

The gelation ability of bhilawanol glycolipids was identified by the “stable to inversion method” in a broad range of organic solvents, water, and vegetable oils. To evaluate the gelation ability, the appropriate amount of gelator and solvent/oil was taken in a vial and sealed. Upon heating the vial, a complete dissolution of the gelator occurred, and the solution became homogeneous. The homogeneous solution was cooled to room temperature, and gelation was observed. In the end, the vial was inverted and investigated; the stage of no gravitational flow in the inverted vial denotes the gelation, “G.” Instead, if it remains in solution, it is referred to as “S”; if it remains as a precipitate, it is indicated as precipitation, “P” and if the gelator does not dissolve upon heating, it is referred to as insoluble (I).



The morphology of the gel obtained from bhilawanol glycolipids was obtained by optical microscopy and scanning electron microscopy (SEM) using a Carl Zeiss AXIO ScopeA1 fluorescent/phase contrast microscope. The xerogel obtained was subjected to X-ray measurement using an Xpert-PRO Diffractometer system. UV/vis spectra were recorded on a Thermo Scientific Evolution 220 UV/visible spectrophotometer. The spectra were recorded in the constant mode between 200 and 700 nm, with a wavelength increment of 1 nm and a bandwidth of 1 nm. Infrared (IR) spectra were recorded in the range of 400–4000  $\text{cm}^{-1}$  using KBr in a PerkinElmer spectrum 100 spectrophotometer. The visco-elastic characteristics of the gel prepared from bhilawanol glycolipids were investigated by carrying out rheological measurements at 23 °C using a stress-controlled rheometer (Anton Paar Modular Compact Rheometer 302) with a 25 mm diameter steel-coated parallel-plate geometry. Rheological measurements for the gel were recorded by placing the gel sample over the parallel plate with 1 mm gap between the plates and subsequently trimming the excess gel.

### Cytotoxicity studies

Human corneal epithelial cells (HCEC) were seeded in 96 well-plates in DMEM-F12 (Lonza, Walkersville, MD) media supplemented with 10% fetal bovine serum (FBS; Lonza, Walkersville, MD), 4  $\mu\text{g mL}^{-1}$  insulin (HiMedia Laboratory, Maharashtra, India) and 20  $\text{ng mL}^{-1}$  of EGF. To test the cytotoxicity, different concentrations of compound **4b** were added to the cells and incubated for 6 h and 24 h at 37 °C in a 5%  $\text{CO}_2$  incubator. The culture media was aspirated, and the wells were washed with sterile  $1\times$  PBS to remove the non-adherent cells. 100  $\mu\text{L}$  of 5  $\text{mg mL}^{-1}$  MTT solution was added to the wells. The plates were incubated further at 37 °C in a 5%  $\text{CO}_2$  incubator for 2 h. The media was removed, 200  $\mu\text{L}$  of DMSO was added and mixed properly, and absorbance was recorded at 595 nm.

### Anti-microbial study

Compound **4b** was dissolved in DMSO at a 20  $\text{mg mL}^{-1}$  concentration. The pathogen was grown in the media (Luria Bertini broth for *P. aeruginosa* and *E. coli*; and Todd Hewitt broth for *S. pneumoniae* to log phase) and then centrifuged at 10000 rpm for 10 min. It was then resuspended in the respective growth media to get the desired concentrations. The pathogen was incubated with different concentrations of **4b** (100, 250, 500, and 1000  $\mu\text{g mL}^{-1}$ ) for 24 h. The growth of the pathogen was determined by recording the absorbance at 600 nm. For the determination of biofilm formation, the culture supernatant was gently removed, and the wells were washed with distilled water to remove any trace of the culture media or the non-adherent pathogen. The biofilm was fixed with 95% methanol for 10 min. After removing methanol, the wells were air dried, and then the biofilm was stained with 0.5% crystal violet for 15 min. The crystal violet was removed, washed with distilled water, 30% acetic acid was added to

the wells, incubated for 10 min to dissolve the crystal violet stain, and absorbance was recorded at 595 nm.

### Curcumin encapsulation into hydrogel and release studies

5 mg of curcumin is added into the hydrogel (CGC: 1.0% wt/v), followed by heating to get a clear yellow solution, and cooled to room temperature. The formation of the composite gel was confirmed by observing no gravitational flow upon test tube inversion. pH-responsive drug release studies were performed in acidic, basic and neutral pH levels. To the composite hydrogel derived from **4b**, 10 mL of acidic buffer (pH = 4) was added, and 1 mL of aliquots were retrieved at different intervals. The concentration of curcumin drug release was monitored by UV-vis spectroscopy by diluting 1.0 mL of the retrieved aliquot to 2.0 mL using double distilled water. The same procedure was applied for basic and neutral pH levels.

## Synthesis

The synthesis of bhilawanol glycolipid consists of three steps: converting bhilawanol to an ester (**2**), then to a hydrazide (**3a**, **3b**), and finally to bhilawanol glycolipid (**4a** and **4b**).

### Synthesis of compound 2

To a stirred solution of bhilawanol (1.0 mmol, **1**) in acetone, 2 mmol of methyl bromoacetate was added in the presence of anhydrous potassium carbonate (3 mmol) and refluxed for 24 h. After confirming the completion of the reaction using TLC, the reaction was stopped, cooled to room temperature, and extracted using ethyl acetate. The desired product was isolated by concentrating the extract using a rotary evaporator.

Isolated as a golden brown viscous liquid; yield = 93%  $^1\text{H}$  NMR (400 MHz,  $\text{CDCl}_3$ )  $\delta$  6.86 (t,  $J$  = 7.9 Hz, 1H), 6.75 (d,  $J$  = 7.7 Hz, 1H), 6.58 (d,  $J$  = 8.1 Hz, 1H), 5.30–5.24 (m, 3H), 4.64 (s, 2H), 4.56 (s, 2H), 2.70–2.59 (m, 3H), 1.96–1.89 (m, 4H), 1.50 (t,  $J$  = 7.2 Hz, 2H), 1.32–1.18 (m, 16H), 0.85–0.78 (m, 3H).  $^{13}\text{C}$  NMR (100 MHz,  $\text{CDCl}_3$ )  $\delta$  173.35, 172.93, 143.24, 129.99, 129.68, 127.89, 121.82, 119.74, 112.70, 68.96, 62.13, 29.79, 29.72, 29.68, 29.55, 29.34, 29.13, 29.10, 27.23, 27.18, 22.69, 22.66, 14.08.

### Synthesis of 3a

To a stirred solution of bhilawanol methyl ester **2** (2.0 mmol) in ethanol, hydrazine hydrate (0.5 mmol) was added and refluxed for 12 h. After confirming the completion of the reaction, as identified by TLC, the reaction was stopped and cooled to room temperature. Upon cooling, the desired product was precipitated, filtered, washed with ethanol, and dried. The off-white amorphous solid obtained was recrystallized using methanol.

Isolated as an off white solid; m.p. 98–100 °C, yield = 93%.  $^1\text{H}$  NMR (400 MHz,  $\text{DMSO-d}_6$ )  $\delta$  9.31 (s, 1H), 9.25 (s, 1H), 6.97 (t,  $J$  = 7.9 Hz, 1H), 6.80 (t,  $J$  = 7.9 Hz, 2H), 5.65–5.12



(m, 1H), 4.51 (s, 2H), 4.37 (s, 2H), 2.62–2.55 (m, 2H), 1.99 (dd,  $J = 12.4, 6.6$  Hz, 2H), 1.50 (s, 2H), 1.26 (d,  $J = 16.4$  Hz, 20H), 0.86 (s, 3H).  $^{13}\text{C}$  NMR (100 MHz,  $\text{CDCl}_3$ )  $\delta$  169.69, 168.24, 149.67, 145.21, 137.25, 130.03, 129.76, 125.11, 123.68, 111.36, 72.01, 67.69, 31.94, 29.88, 29.77, 29.71, 29.67, 29.64, 29.59, 29.55, 29.44, 29.37, 27.24, 14.13. HRMS (ESI,  $m/z$ ):  $[\text{M} + \text{H}]^+$  calcd. for  $\text{C}_{25}\text{H}_{42}\text{N}_4\text{O}_4$ : 462.3206; found 463.3289.

### Synthesis of 3b

To a stirred solution of bhilawanol methyl ester 2 (1.0 mmol) in ethanol, hydrazine hydrate (4.0 mmol) was added and refluxed for 24 h. Initially, the formation of 3a was observed, and refluxing was continued for about 24 h, generating the corresponding saturated compound 3b. After confirming the completion of the reaction, as identified by TLC, the reaction was stopped and the reaction mixture was cooled to room temperature. Upon cooling, the desired product was precipitated, filtered, washed with ethanol, and dried. The white amorphous solid obtained was recrystallized using methanol.

Isolated as a white crystalline solid; m.p. 104–106 °C; yield = 90%.  $^1\text{H}$  NMR (400 MHz,  $\text{CDCl}_3$ )  $\delta$  7.98 (s, 1H), 6.98 (t,  $J = 7.8$  Hz, 1H), 6.81 (d,  $J = 7.7$  Hz, 1H), 6.66 (d,  $J = 7.2$  Hz, 1H), 4.47 (d,  $J = 34.5$  Hz, 6H), 2.84 (s, 5H), 2.24 (t,  $J = 7.6$  Hz, 1H), 1.50 (s, 3H), 1.21 (d,  $J = 17.4$  Hz, 37H), 0.81 (t,  $J = 6.7$  Hz, 5H).  $^{13}\text{C}$  NMR (100 MHz,  $\text{CDCl}_3$ )  $\delta$  169.66, 168.20, 149.67, 145.21, 137.27, 125.11, 123.69, 111.35, 72.02, 67.71, 31.93, 30.75, 29.89, 29.70, 29.64, 29.55, 29.37, 22.70, 14.13. HRMS (ESI,  $m/z$ ):  $[\text{M} + \text{H}]^+$  calcd. for  $\text{C}_{25}\text{H}_{44}\text{N}_4\text{O}_4$ : 464.3363; found: 465.3448.

### Synthesis of 4a and 4b

In an RB flask, one or two drops of pyridine were added to a methanolic solution of glucono- $\delta$ -lactone (1 mmol) and bhilawanol hydrazide 3a or 3b (0.5 mmol) and refluxed for 24 h. After the reaction was completed, as identified by TLC, it was stopped and cooled to room temperature. A sticky solid was filtered and washed very well with methanol to ensure the complete removal of pyridine. The pure product suitable for self-assembly studies was obtained by recrystallization using methanol.

**Compound 4a.** Isolated as a white solid; m.p. 103–105 °C; yield = 87%;  $^1\text{H}$  NMR (400 MHz,  $\text{DMSO-d}_6$ )  $\delta$  10.17 (s, 1H, -NH), 9.96 (s, 1H, -NH), 9.64 (d,  $J = 7.3$  Hz, 2H, -NH), 6.98 (t,  $J = 7.9$  Hz, 1H, Ar-H), 6.86 (d,  $J = 8.2$  Hz, 1H, Ar-H), 6.80 (d,  $J = 7.5$  Hz, 1H, Ar-H), 5.46 (t, 2H, sac-H), 5.33 (s, 1H, alk-H), 4.67 (s, 1H, sac-H), 4.65–4.58 (m, 1H sac-H), 4.56–4.50 (m, 3H, sac-H), 4.47 (s, 2H, sac-H), 4.36 (d,  $J = 1.8$  Hz, 4H, sac-H), 4.15 (dt,  $J = 5.8, 3.9$  Hz, 2H, sac-H), 3.94 (dq,  $J = 6.8, 3.4$  Hz, 2H, sac-H), 3.64–3.56 (m, 2H, sac-H), 3.55–3.47 (m, 4H, sac-H), 3.39 (q,  $J = 5.9$  Hz, 4H, sac-H), 2.65–2.58 (m, 2H, -CH<sub>2</sub>), 1.99 (d,  $J = 5.6$  Hz, 2H, -CH<sub>2</sub>), 1.52 (s, 2H, -CH<sub>2</sub>), 1.26 (d,  $J = 15.9$  Hz, 18H, -CH<sub>2</sub>), 0.86 (dd,  $J = 6.6, 4.4$  Hz, 3H, -CH<sub>3</sub>).

$^{13}\text{C}$  NMR (100 MHz,  $\text{DMSO-d}_6$ )  $\delta$  171.40, 171.08, 167.41, 167.00, 150.93, 145.78, 136.49, 130.14, 130.09, 124.46, 122.82,

112.25, 73.51, 73.39, 72.28, 72.17, 72.08, 71.97, 71.22, 70.87, 70.81, 66.91, 63.89, 63.85, 31.76, 31.60, 29.63, 29.55, 29.52, 29.48, 29.18, 28.74, 27.07, 22.56, 14.42. HRMS (ESI,  $m/z$ ):  $[\text{M} + \text{H}]^+$  calcd. for  $\text{C}_{37}\text{H}_{62}\text{N}_4\text{O}_{16}$ : 818.4161; found: 841.4053.

**Compound 4b.** Isolated as a white solid; m.p. 117–119 °C; yield = 82%;  $^1\text{H}$  NMR (400 MHz,  $\text{DMSO-d}_6$ )  $\delta$  10.17 (s, 1H, -NH), 9.97 (s, 1H, -NH), 9.65 (s,  $J = 7.3$  Hz, 2H, -NH), 6.98 (t,  $J = 7.9$  Hz, 1H, Ar-H), 6.83 (dd,  $J = 21.6, 6.9$  Hz, 1H, Ar-H), 6.82 (dd,  $J = 21.6, 6.9$  Hz, 1H, Ar-H), 5.47 (t,  $J = 5.6$  Hz, 2H, sac-H), 4.67 (s, 1H, sac-H), 4.64 (s, 1H, sac-H, sac-H), 4.56 (d,  $J = 5.0$  Hz, 1H, sac-H), 4.53 (s, 1H, sac-H), 4.48 (s, 2H, sac-H), 4.36 (s, 4H, sac-H), 4.24–4.12 (m, 2H, sac-H), 3.93 (s, 2H, sac-H), 3.58 (d,  $J = 2.8$  Hz, 2H, sac-H), 3.51 (d,  $J = 5.7$  Hz, 4H, sac-H), 3.37 (s, 4H, sac-H), 2.68–2.57 (t, 2H, -CH<sub>2</sub>), 1.52 (m, 2H, CH<sub>2</sub>), 1.26 (d,  $J = 14.8$  Hz, 23H, CH<sub>2</sub>), 0.86 (t,  $J = 6.8$  Hz, 3H, -CH<sub>3</sub>).

$^{13}\text{C}$  NMR (100 MHz,  $\text{DMSO-d}_6$ )  $\delta$  171.50, 171.41, 167.44, 167.02, 150.92, 145.76, 136.49, 124.47, 122.83, 112.23, 73.51, 72.28, 72.16, 71.96, 70.86, 63.89, 63.84, 31.76, 29.53, 29.48, 29.18, 22.57, 14.43. HRMS (ESI,  $m/z$ ):  $[\text{M} + \text{H}]^+$  calcd. for  $\text{C}_{37}\text{H}_{64}\text{N}_4\text{O}_{16}$  = 820.4317; found: 843.4231.

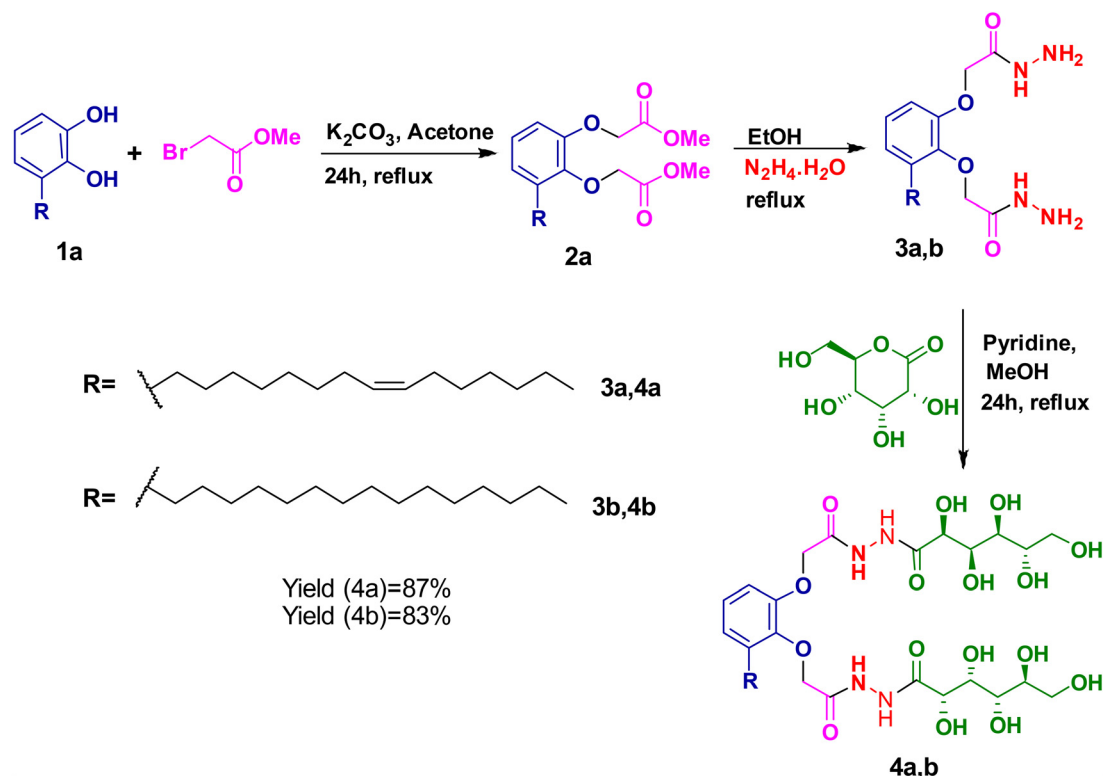
## Results and discussions

### Synthesis of glycolipids

Hydrogels are cross-linked 3-dimensional materials with trapped water molecules, which display unique physical and chemical properties.<sup>29</sup> This class of biocompatible materials is highly appealing for a wide range of applications such as drug delivery, gene therapy, and tissue engineering.<sup>30–33</sup> Generally, a biocompatible system is non-toxic to living cells and penetrates smoothly in tissues; hence, DMSO–water systems are considered solubilizing agents in drug discovery and delivery applications.<sup>34</sup> Recent research on biotechnology and pharmaceuticals has revealed that hydrogels are one of the most efficient drug delivery methods, with negligible cytotoxic effects and good bio-compatibility.<sup>35</sup> In the present study, we developed a multifunctional hydrogel system displaying stimuli-responsive drug delivery for curcumin, one of the traditional natural drug molecules, and anti-microbial properties. Owing to the hydrophobic nature of curcumin, low bioavailability is displayed, and a suitable delivery system is necessitated. Even though only a handful of literature on the delivery of curcumin is available, small molecular glycolipid-based hydrogels for the delivery of curcumin in a stimuli-responsive manner with antimicrobial properties have not been reported.<sup>36–39</sup>

For glycolipid synthesis, we selected bhilawanol as one of the starting materials because of its traditional medicinal uses, such as antineoplastic, antiarthritic, immunomodulatory, anthelmintic, and hypocholesterolemia activities. Bhilawanol methyl ester was prepared from bhilawanol and methyl bromo acetate in the presence of  $\text{K}_2\text{CO}_3$  under reflux conditions.<sup>40</sup> The bhilawanol methyl ester thus obtained was treated with hydrazine under reflux conditions, yielding the corresponding bhilawanol hydrazide in excellent yields even without the need





**Scheme 1** Synthesis of bhilawanol-based glycolipids, **4a** and **4b**.

for column chromatography (Scheme 1).<sup>31</sup> The corresponding saturated version, **3b**, was synthesized, and the formation of the desired product was confirmed by NMR spectral analysis. The reaction of bhilawanol hydrazides **3a** and **3b** with gluconolactone in methanol and pyridine furnished the *N*-(bhilawanol hydrazide)-*D*-gluconamides, **4a** and **4b**, in good yields (Scheme 1). The formation of **4a** and **4b** was confirmed by NMR and mass spectroscopy (refer ESI†).

### Gelation studies

Despite the limitations of polymer-based gels, such as irreversibility, difficulty in processability, lack of fine-tuning, and high molecular weight, they were widely used to fabricate hydrogel-based drug delivery systems. To overcome these limitations, recently, the employment of small amphiphilic molecules that undergo supramolecular self-assembly has gained broad interest in the construction of smart delivery systems *via* intermolecular interactions to form 3D aggregates entrapping the solvents. The introduction of advancements in pharmaceutical technology by designing a new gelator based on clinically significant molecules is crucial. With bhilawanol glycolipid on hand, we further investigated the gelation behavior in various solvents and oils using the “stable to inversion method”.<sup>41</sup> A broad range of solvents, such as water, vegetable oils, ethylene glycol, polyethylene glycol (PEG), and some other polar and non-polar organic solvents, were used for gelation studies. Interestingly, bhilawanol glycolipids **4a** and **4b** displayed gelation in

DMSO–CHCl<sub>3</sub> (3 : 7) and DMSO–water (4 : 6) with CGC of 2.0, 1.0, 1.5 and 1.0% wt/v, respectively (Table S1†). Investigation of the gelation behaviour of bhilawanol glycolipid displayed uniqueness in forming a gel in DMSO-based systems. A complete dissolution is observed in DMSO, which renders a transparent solution upon heating and cooling to room temperature. At room temperature, the further addition of either hydrophilic solvent (H<sub>2</sub>O) or a hydrophobic solvent (CHCl<sub>3</sub>) delivered a gel by molecular self-assembly at room temperature (Fig. 1a). It is worth mentioning that this type of room-temperature gelation is one of the important criteria for tissue engineering, cell proliferation, and other advanced biotechnological research. The thermoreversible nature of the gel (T<sub>g</sub>) formed by **4a** and **4b** in DMSO–water (4 : 6) was identified by repeated heating and cooling cycles and found to be 106 and 118 °C, respectively. An increase in the concentration of gelator **4b** enhances the T<sub>g</sub>, indicating the tunability of gel strength (Fig. S19†). It is worth mentioning that the hydrogel obtained from compound **4b** displayed better CGC and exceptional gel strength when compared to **4a**. The presence of kink in compound **4a** interferes with the molecular assembly process; hence, increased CGC and decreased gel strength were observed.

### Morphology and assembly mechanism

Molecular aggregation of bhilawanol glycolipid in DMSO–water, a biocompatible system to generate a self-assembled fibrillar network (SAFIN), is one of the interesting features in



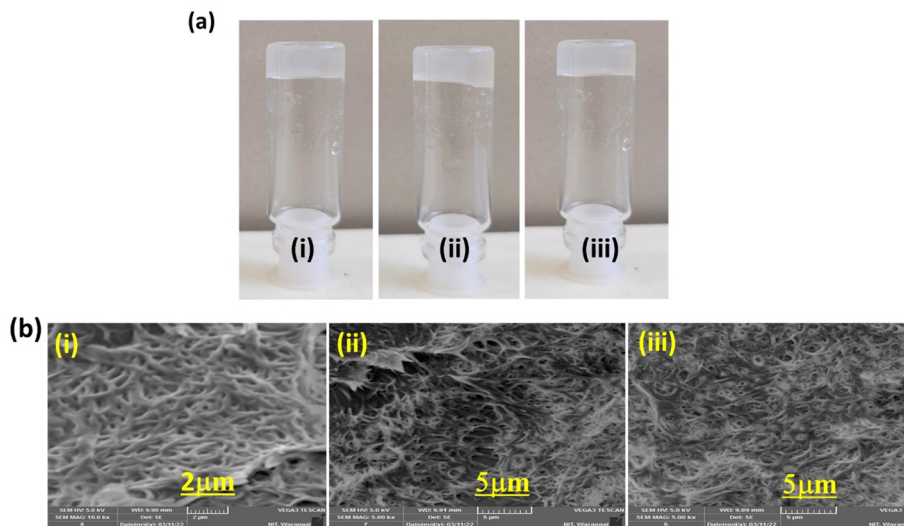


**Fig. 1** (a) Gel images of (i) compound **4a** and (ii) **4b** in DMSO–chloroform (3 : 7 v/v) and (iii) **4b** in DMSO–water (4 : 6 v/v). (b) (i–iii) SEM images of the hydrogel formed by **4b**.

supramolecular chemistry. The assembly of molecules due to the intermolecular interactions displayed by hydroxyl and amide groups,  $\pi$ – $\pi$  stacking, and other hydrophobic interactions are responsible for the formation of SAFIN. We recorded the optical and scanning electron microscopy (SEM) images of the hydrogel of **4b** for morphological studies. Optical microscopy investigation of the hydrogel formed by **4b** in DMSO–water revealed the existence of distinctly different microstructures; however, it did not provide any conclusive architecture (Fig. S18†). We performed SEM analysis to understand the distinct morphology shown by the hydrogel deeply, which revealed the formation of a dense fibrillar network with width ranging from 100 to 200 nm (Fig. 1b).

Molecular assembly of 3D materials is a fascinating research area and has received attention in biomaterials field because of its tunable properties arising at the molecular level. The various intermolecular interactions governing the assembly process deliver clear-cut molecular design parameters correlating to the crystallization process. Variable-temperature NMR studies of the gel reveal the influence of various groups in molecular assembly. Fortunately, compound **4b** displayed gelation in the DMSO–H<sub>2</sub>O system, facilitating the molecular-level investigation of intermolecular interactions. The <sup>1</sup>H NMR spectrum of compound **4b** in DMSO-d<sub>6</sub> displayed peaks at  $\delta$  = 10.17, 9.97, and 9.66 ppm corresponding to the NH protons,  $\delta$  = 7.00–6.80 ppm corresponds to aromatic protons,  $\delta$  = 5.74–3.50 ppm for the carbohydrate unit and –OCH<sub>2</sub> protons, and  $\delta$  = 2.64–0.84 ppm corresponding to the hydrophobic alkyl chain (Fig. 2a). Since our compound forms a gel in a DMSO–H<sub>2</sub>O system, upon the addition of D<sub>2</sub>O, a clear transparent gel formation was observed at room temperature, which was then used to record the variable temperature NMR spectrum. The <sup>1</sup>H NMR spectra of the gel formed in DMSO-d<sub>6</sub>–D<sub>2</sub>O at 60 °C displayed the broadening of signals corresponding to the carbohydrates, the disappearance of the exchangeable proton and aromatic peaks, along with the infinitesimally small shifts in the peaks

corresponding to carbohydrates. It is worth mentioning that a gradual increase in temperature occurred from 60 to 90 °C. As shown in Fig. 2a, gel-to-sol transition was observed. Upon the increase in temperature, signals corresponding to the aromatic peaks at about  $\delta$  = 7.0 ppm started displaying signals with an upfield shift, and signals corresponding to the carbohydrates were well resolved. NMR studies clearly reveal the participation of various groups in molecular self-assembly, especially when molecules were packed so that the hydrophilic sugar unit was projected outwards and the hydrophobic aryl and alkyl chains were buried inside the assembled structure. Generally, the electronic environment of a proton decides the chemical shift in NMR. Any phenomenon that increases the electron density of a proton generates an increased induced magnetic field ( $B_{\text{induced}}$ ) on the proton, which effectively opposes the applied magnetic field ( $B_0$ ). Thus, such an environment feels a less applied magnetic field and hence a relatively lower frequency is enough to cause resonance in such protons. In Fig. 2a, upon self-assembly, an upfield shift in the signals of the aryl proton reveals the involvement of  $\pi$ – $\pi$  stacking. In addition, NMR studies establish the existence of strong H-bonding to generate the hydrogel.

To understand the self-assembly mechanism, molecular-level insights are necessitated. Various intermolecular interactions such as hydrogen bonding,  $\pi$ – $\pi$  stacking, anion– $\pi$ , cation– $\pi$  and van der Waals displayed by a molecule play a crucial role in the assembly mechanism. Fourier transform infrared spectroscopy is the best tool for studying intermolecular interactions with respect to functional groups. We recorded the attenuated total reflectance Fourier transform infrared (ATR-FTIR) spectrum for the amorphous compound **4b** and its xerogel (Fig. 2b). The characteristic peak in the FTIR spectra of **4b** in the amorphous state displayed peaks at 3316, 3229, 2851, 1697, 1663, and 1096 cm<sup>-1</sup>, which correspond to –OH, –NH, –CH (alkane), –C=O, and –C–O (secondary alcohol), respectively. Typically, in the amorphous state, various functional groups, alkyl moiety, and



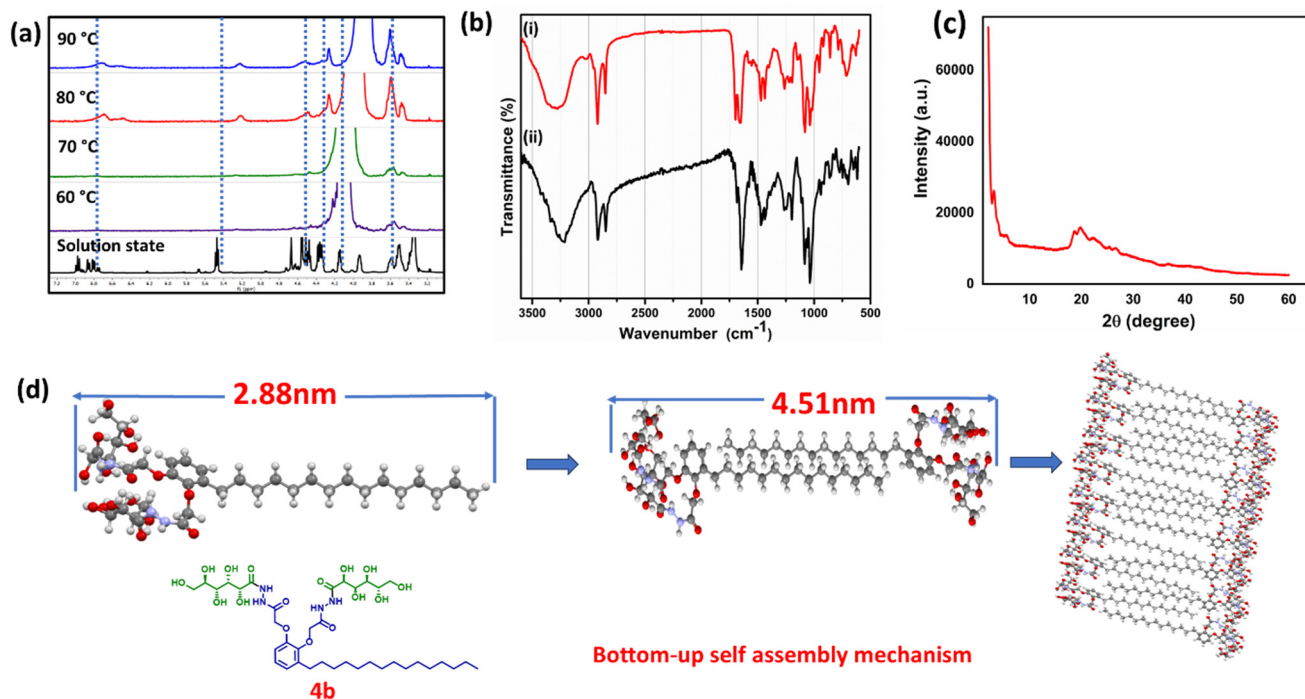


Fig. 2 (a) Variable-temperature  $^1\text{H}$  NMR studies of the hydrogel derived from **4b**. (b) FTIR spectra of the hydrogel of **4b** in the amorphous and assembled states. (c) XRD pattern of the xerogel of **4b**. (d) Proposed bottom-up self-assembly mechanism.

aryl systems arrange randomly in a 3-dimensional lattice, with minimal potential for intermolecular aggregation. Interestingly, compound **4b**, in its xerogel state, exhibited a distinct molecular arrangement influenced by intermolecular interactions, which was directly reflected in the ATR-IR analysis. In the xerogel state, peaks observed at 3285, 3224, 2846, 1684, 1652, and 1083  $\text{cm}^{-1}$  correspond to  $-\text{OH}$ ,  $-\text{NH}$ ,  $-\text{CH}$  (alkane),  $-\text{C}=\text{O}$ , and  $-\text{C}-\text{O}$  (secondary alcohol), respectively. A careful analysis of IR data revealed that the characteristic peaks of functional groups responsible for intermolecular interaction, such as  $-\text{OH}$ ,  $-\text{NH}$ ,  $-\text{C}=\text{O}$ , and  $-\text{C}-\text{O}$  (secondary alcohol), displayed a lower region shift and were in good accordance with the principle of IR spectroscopy (Fig. 2b). Small angle XRD studies were also carried out to further explore the molecular packaging in the xerogel of compound **4b**, given in Fig. 2c. Predicting the molecular arrangement within the supramolecular gel is exceptionally challenging as the structure and characteristics depend on the geometry and arrangement of building blocks in a three-dimensional lattice. Nonetheless, by understanding the intermolecular interactions among the gelator from FTIR analysis, we can predict the packing through the small angle-XRD (SA-XRD) technique. The xerogel obtained from compound **4b** displayed  $2\theta = 1.96^\circ$ ,  $2.26^\circ$ ,  $3.11^\circ$ ,  $3.92^\circ$ ,  $4.66^\circ$ , and  $5.44^\circ$  corresponding to the interplanar spacing ( $d$ -spacing) at 4.51, 3.91, 2.84, 2.25, 1.90, and 1.62 nm, respectively. It is worth mentioning that peaks displayed at  $18.63^\circ$ ,  $19.80^\circ$ ,  $25.35^\circ$ , and  $26.58^\circ$  correspond to  $\pi$ - $\pi$  stacking and hydrogen bonding, respectively (Fig. 2c). Intermolecular interactions facilitate molecular self-assembly, creating a 3D fibrillar network architecture measuring a length of 4.51 nm, as determined by

XRD, which is higher than the end-to-end molecular length of compound **4b** (Fig. 2d).

The end-to-end molecular length of **4b** is 2.88 nm, calculated from the energy-minimized structure. XRD analysis clearly reveals the existence of a double-layer assembly stabilised by intermolecular interactions. As evidenced by NMR, FTIR and XRD studies, the intermolecular hydrogen bonding between the amide, hydroxyl groups and van der Waals forces facilitate the molecular self-assembly, thereby forming a 3 dimensional network architecture. During the process of gelation, the solvent is trapped in the 3D network structure, thereby forming the gel.

### Rheological studies

Rheological measurements were carried out to study the macroscopic properties of gels, such as viscoelastic, injectable, self-healing, thixotropic behaviors, and mechanical strength, in response to the applied force. The extent of deformation of a material from its original structure in response to applied force could be identified by rheological measurement. The rheological properties of the gel directly reflect the flow characteristics and elastic behavior, which generally depend upon the gel microstructure, strength, and solvent interaction. The rheology of gels was identified by measuring the storage modulus  $G'$  (elastic) and loss modulus  $G''$  (viscous) with respect to the applied external stimulus. The deformation of this viscoelastic material in response to stress or strain is due to changes in the internal morphology or changes in the supramolecular arrangement of small or macromolecules (Fig. 3). To realise the practical utility of these gels in biomedical applications, a clear understanding of



the physical properties of the molecular architecture in the gel is required. The rheology of the hydrogel formed by compound **4b** is given in Fig. 3a–f. In the frequency sweep test, the linear increase in both  $G'$  and  $G''$  with increasing values of applied frequency and also a higher value of  $G'$  than  $G''$  indicated the stability and good tolerance towards the external forces. In the strain sweep test, the higher values of  $G'$  against  $G''$  reveal the good mechanical strength of the gels. The thixotropy (a step strain) experiment depicts exceptional mechanical behavior as well as the structural recovery of the hydrogel due to the application of different strains to the gel. By applying a constant strain of 100%, the 3D network architecture holding the solvent gets disturbed and the gel experiences a reduction in strength. However, upon reducing the strain to 0.1%, the gels regained the viscosity and returned to their gel state. Through a sequence of continuous strain ramp-up and ramp-down experiments, we observed a gradual deterioration in the gel's structural integrity as the strain increased. However, the original state promptly recovered as the strain was eased back to 0.1%. It is worth mentioning that upon heating to 150 °C and cooling to RT, a sol-to-gel transition was observed even after 15 cycles, demonstrating the stability and thermal processability of the gel.

### Encapsulation and stimuli-responsive drug release

For centuries, traditional and complementary medicines have been an inherent source of health in communities. Curcumin is an active pharmaceutical compound isolated from turmeric,

one of the traditional natural medicines.<sup>42</sup> Although curcumin has significant benefits, such as anti-cancer, cardiovascular diseases, inflammatory and neurological disorders, and Alzheimer's disease, its clinical implications are limited because of poor solubility, physicochemical instability, rapid metabolism, and poor pharmacokinetics.<sup>43</sup> Owing to this, several research groups are actively involved in developing biocompatible curcumin formulations for various human diseases. Among the various methods, the encapsulation of curcumin in hydrogel and its stimuli-responsive release are highly fascinating. In the present studies, curcumin is encapsulated into a hydrogel by a simple co-gelation method. Adding 5.0 mg of curcumin onto the preformed hydrogel (1.0% wt/v), followed by heating and cooling to room temperature, generated the curcumin-encapsulated hydrogel. Upon encapsulation of curcumin, a change in the morphology of the gel fibres is observed because of the intercalation of curcumin in the hydrophobic part of the gel fibres. The higher loading of curcumin is observed because of the entrapment of curcumin in the 3D fibrous network. SEM analysis of the curcumin-encapsulated hydrogel revealed the existence of morphological change because of the intercalation of curcumin into the fibrous network structure (Fig. 4).

In the past decade, researchers have pioneered studies on hydrogels displaying stimuli-responsive behavior, especially for drug formulation, tissue engineering, and regenerative medicine.<sup>44,45</sup> This class of smart biomaterials holds promise in modern medicine, and it is crucial to generate a library of smart

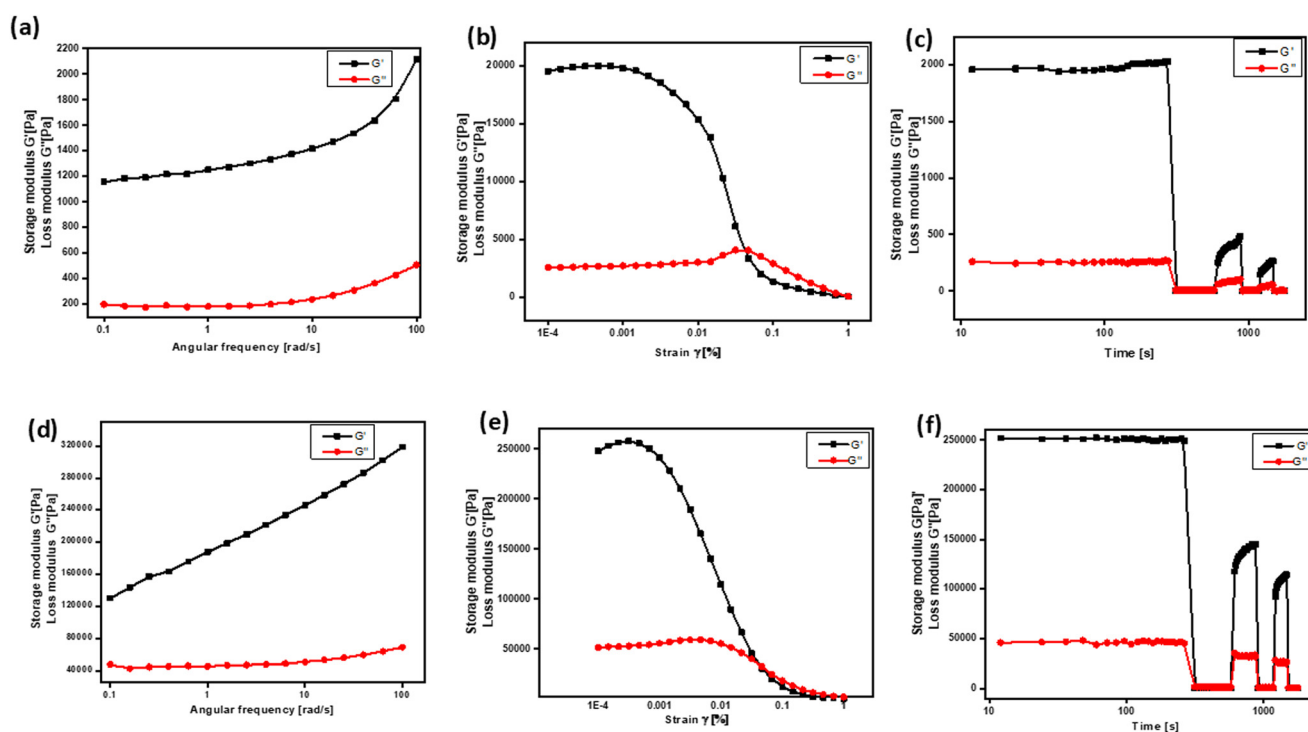
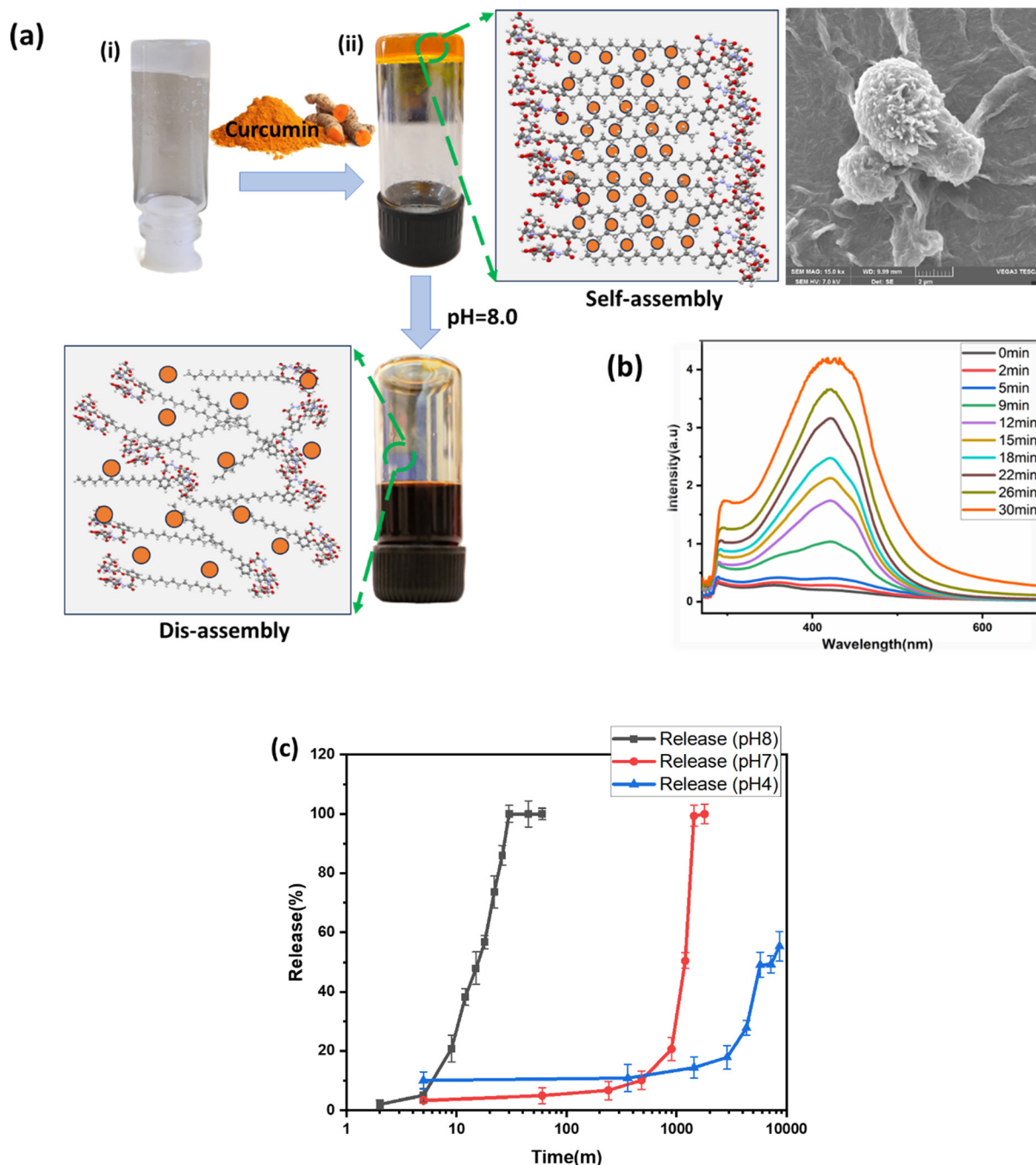


Fig. 3 Angular frequency and strain amplitude dependence of  $G'$  and  $G''$  of the gel formed by **4b** (a and b) in DMSO-CHCl<sub>3</sub> and (d and e) DMSO-H<sub>2</sub>O, respectively. Thixotropic studies using continuous strain ramp-up and ramp-down measurements of the gel formed by **4b** (c) in DMSO-CHCl<sub>3</sub> and (f) DMSO-H<sub>2</sub>O, respectively.





**Fig. 4** (a) Pictorial representation of curcumin loading into the hydrogel formed by **4b** and its release profile. (i) Image of hydrogel formed by **4b**. (ii) Image of curcumin-loaded hydrogel formed by **4b**. (b) UV-visible spectra of drug release at different time intervals in the presence of a buffer solution. (c) Curcumin release profile of the hydrogel derived from **4b**.

delivery systems and conduct a detailed investigation.<sup>46</sup> A natural drug, curcumin, was encapsulated in the biocompatible hydrogel and characterized entirely. After complete characterization, the release profile of the entrapped curcumin in the hydrogel was studied in the acidic, neutral, and basic pH. The gel exhibited curcumin release in a basic medium (pH = 8.0). The gel releases the drug in a time period of 30 min, while maintaining longer stability for over 24 hours with little leaching of surface-entrapped curcumin in a neutral pH

medium. A pH-dependent release kinetics study revealed the steady release of curcumin at pH = 8, whereas at a neutral pH, leaching of the encapsulated drug from the gel surface was observed without gel-to-sol transition. It is worth mentioning that using an acidic pH 4 solution, the encapsulated curcumin was released slowly without losing its 3D architecture for more than five days. This mechanism of curcumin encapsulation within the gel can be attributed to its hydrophobic nature. In the hydrogelation, compound **4b** assembles in such a way that



the polar sugar molecules orient themselves outward, and the hydrophobic part intercalates to generate a fibrillar sheet-type architecture. NMR, FTIR, and XRD analysis revealed that the fibre's core is built of intercalated hydrophobic units, and the surface is hydrophilic and stabilized by intermolecular H-bonding. During curcumin encapsulation, the hydrophobic curcumin molecule gets encapsulated in the hydrophobic core of the fibre. pH as the stimuli-responsive release of curcumin could be explained based on the structural tuning of the gelator, which results in gel-to-sol transition, followed by the release of a drug. The direct abstraction of the acidic proton of hydrazide core by the basic buffer resulted in a significant change in the 3D structure and intermolecular H-bonding, facilitating gel-to-sol transition.<sup>47</sup> In addition, the excellent solubility of curcumin under a basic pH solution than in an acidic pH may explain its faster release in the basic environment. Another factor influencing the slower release in acidic pH condition is the higher degree of protonation of curcumin and the inertness of the gelator.<sup>48</sup> This phenomenon can also be attributed to the exchange of solvent along with encapsulated curcumin and swelling of the porous structure because of the tuning of H-bonding in the molecular structure. Designing a system holding various functional groups could display smartness in tuning its architecture without undergoing any molecular transformation. A literature review revealed that a basic pH is developed in the body because of respiratory, metabolic, hypochloremic and hypokalemic alkalosis, and acidic pH is observed in the tumor microenvironment. The reported system would be one of the potential candidates for basic pH stimuli-responsive delivery of drugs and transdermal drug delivery, also known as patch delivery systems and controlled delivery in tumor sites.<sup>49,50</sup> Further, the hydrogels' drug release under basic pH was examined using UV-vis spectroscopy (Fig. 4b). The time-dependent release of encapsulated and intercalated curcumin drugs was observed at pH 8.0. The UV-vis spectra of aliquots collected at a time interval are displayed in Fig. 4. The time-dependent UV-vis spectra corresponding to neutral and acidic pH are provided in Fig. S20 (ESI†). The curcumin release profile in different pH environments is illustrated in Fig. 4c. Under basic pH conditions, curcumin is rapidly released, reaching saturation within 30 minutes. In contrast, a slow drug release profile is observed initially in neutral and acidic pH conditions. In the later stage, a rapid release profile is observed, which is attributed to the slow penetration of the buffer, followed by the disassembly of the gelator.

### Cell cytotoxicity assay

The feasibility of utilizing the smart stimuli-responsive hydrogel is based on the cytotoxicity of the gelator molecule. To evaluate the cytotoxicity of hydrogelator **4b** on the metabolic activity of cells, HCEC were incubated with 400  $\mu\text{g mL}^{-1}$  of the compounds, and the cell viability and cell cytotoxicity were checked by the MTT assay, as given in Fig. 5. Cytotoxic studies represent the initial phase in assessing the cytotoxicity of substances, particularly bioactive compounds and plant extracts. Minimal to

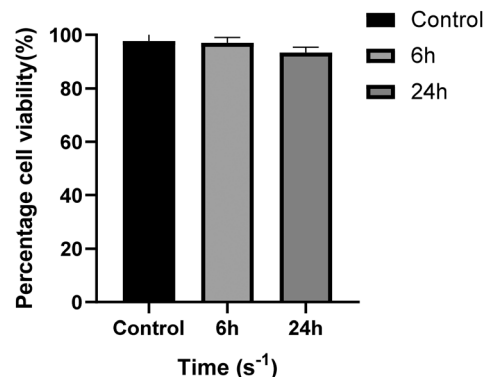


Fig. 5 Cytotoxicity studies of compound **4b**.

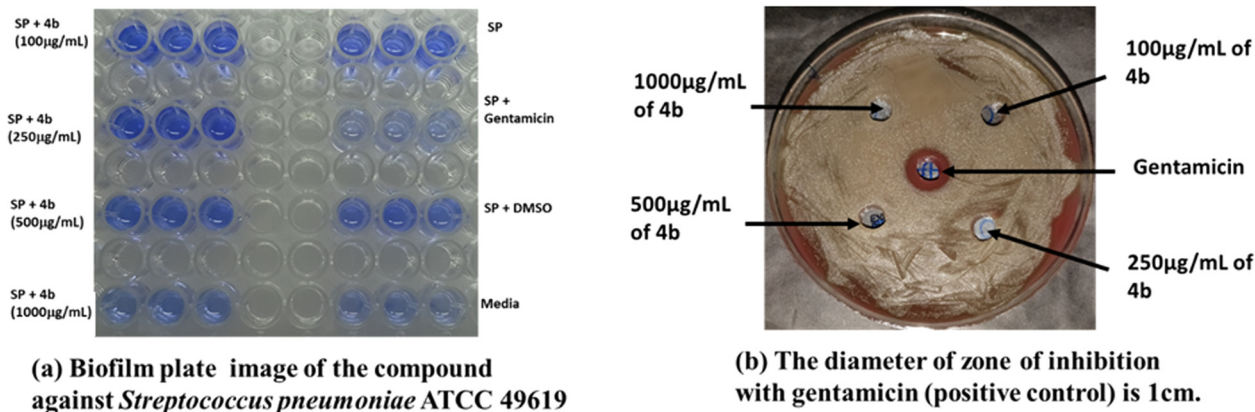
negligible cytotoxicity is essential for successfully utilizing these compounds in pharmaceutical and cosmetic formulations.<sup>51</sup> It was found from the cytotoxic studies that the percentage of cell viability is almost 100% after an incubation period of 6 h and more than 90% after 24 h of incubation of HCEC with 400  $\mu\text{g mL}^{-1}$  of compound **4b**. The good percentage of cell viability (90%) at 1000  $\mu\text{g mL}^{-1}$  of compound **4b** clearly displays the non-cytotoxic behavior of **4b** towards the cells.

### Microbial growth and biofilm assay

Xu and coworkers have discussed the application of supramolecular hydrogelators as molecular biomaterials, which address societal requirements.<sup>52</sup> Recently, Nayak and coworkers highlighted the availability of a diverse class of glycolipid-based gels and their potential biological properties.<sup>53</sup> It is worth mentioning that sugar-based monoesters, rhamnolipids, sophorolipids, and other sugar-derived lipids display promising antimicrobial properties and show significance in eradicating biofilm.<sup>54–59</sup> Traditionally, bhlawanol is used in Ayurvedic medicine.<sup>60</sup> To evaluate the multifunctional nature of the hydrogel, we investigated the *in vitro* antibacterial and antibiofilm activities.<sup>61,62</sup> In our study, we assessed the antibiofilm efficacy of compound **4b** in its amorphous state using the agar diffusion method against *Streptococcus pneumoniae* (Fig. 6b), *P. aeruginosa*, and *E. coli*. Concentration-dependent antibacterial and antibiofilm assays of compound **4b** revealed significant inhibition of biofilm growth against Gram-negative *P. aeruginosa* by 30% at a concentration of 1000  $\mu\text{g mL}^{-1}$ , as depicted in Fig. S21.† When tested against Gram-positive *Streptococcus pneumoniae*, compound **4b** demonstrated antibiofilm activity at a concentration of 1000  $\mu\text{g mL}^{-1}$ , resulting in a 70% reduction in biofilm formation, closely approximating the positive control (Fig. 6), displaying promise in the eradication of the biofilm formed by *Streptococcus pneumoniae* ATCC 49619 strains. Conversely, no inhibition of growth or biofilm was observed for *E. coli* (Fig. S22†).

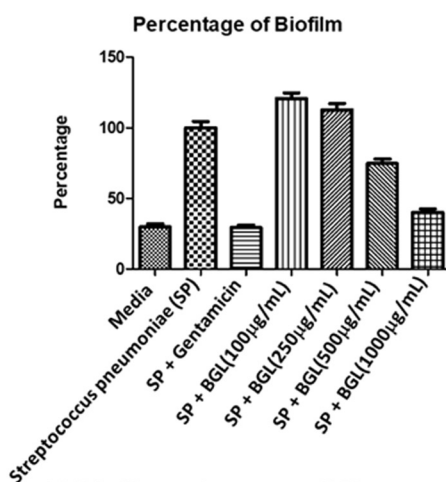
A detailed investigation revealed the potential of compound **4b** against *Streptococcus pneumoniae* ATCC 49619, a Gram-positive bacterium that is very common in history and a highly opportunistic pathogen to humans, animals,





(a) Biofilm plate image of the compound against *Streptococcus pneumoniae* ATCC 49619

(b) The diameter of zone of inhibition with gentamicin (positive control) is 1 cm.



(c) Biofilm resistance at different concentration

Fig. 6 (a) and (b) Antibiofilm activity of compound **4b** against the bacterial pathogen *Streptococcus pneumoniae* ATCC 49619. (c) Percentage of antibiofilm activity at various concentrations.

and plants. In 2017, WHO released a list of bacteria needing urgently developed antibiotics, categorising them as critical, high, and medium priority groups. *Streptococcus pneumoniae* is a medium-critical pathogen as it is a penicillin-resistant pathogen.<sup>63</sup> In the late 1960s, researchers detected the penicillin-resistant and multi-resistant strains of *Streptococcus pneumoniae* and found them to be a major health concern worldwide, including sepsis, bacteremia, meningitis, and community-acquired pneumonia (CAP).<sup>64</sup> Antimicrobial investigation revealed the potential of compound **4b** in combating biofilms formed by *Streptococcus pneumoniae*. Due to their colonial state, biofilms are usually stronger and more antibiotic-resistant.<sup>65</sup> Compound **4b** has almost an equal effect to that of the standard positive control, as shown in Fig. 6c.<sup>66–68</sup> The biofilm formed was determined by measuring the absorbance at 590 nm. Fig. 6a–d represents the pathogen's growth using the agar diffusion method and concentration and time-dependent antibacterial and antibiofilm studies of the compound **4b** against *Streptococcus pneumoniae* ATCC 49619.<sup>69,70</sup> While no change

was seen in the growth of *S. pneumoniae*, compound **4b** efficiently reduced biofilm formation significantly.

## Conclusion

In summary, multifunctional glycolipids were synthesized from biologically significant natural molecules, bhlawanol, and carbohydrates in good yields. Detailed gelation studies of glycolipids revealed hydrogel formation by the formation of a 3D fibrous architecture using a bottom-up assembly process. The molecular-level self-assembly mechanism was thoroughly investigated using various spectral techniques. Rheological measurements ascertained the potential of hydrogel in biomedical applications. This biocompatible hydrogel could encapsulate a natural drug, curcumin, and deliver it in a stimuli-responsive manner. Interestingly, the reported glycolipid displayed significant potential in selectively compacting the biofilm formed by *Streptococcus pneumoniae*. Thus, the reported multifunctional hydrogel derived from bhlawanol-based glycolipid could be a potential candidate in pharmaceuticals and medicine.



## Data availability

The complete data supporting this article have been included as part of the ESI.†

## Author contributions

The manuscript was written with the contributions of all authors, and all authors have approved the final version.

## Conflicts of interest

There are no conflicts to declare.

## Acknowledgements

We greatly acknowledge the financial support from the SERB (sanction order no: CRG/2023/002466) and DST FIST (SR/FST/CS-II/2018/65). The authors thank the National Institute of Technology Warangal for the infrastructure facilities.

## References

- D. Liu, F. Yang, F. Xiong and N. Gu, The Smart Drug Delivery System and Its Clinical Potential, *Theranostics*, 2016, **6**(9), 1306–1323, DOI: [10.7150/thno.14858](https://doi.org/10.7150/thno.14858).
- T. C. Ezike, U. S. Okpala, U. L. Onoja, C. P. Nwike, E. C. Ezeako, O. J. Okpara, C. C. Okoroafor, S. C. Eze, O. L. Kalu, E. C. Odoh, U. G. Nwadike, J. O. Ogbodo, B. U. Umeh, E. C. Ossai and B. C. Nwanguma, Advances in Drug Delivery Systems, Challenges and Future Directions, *Heliyon*, 2023, **9**, e17488, DOI: [10.1016/j.heliyon.2023.e17488](https://doi.org/10.1016/j.heliyon.2023.e17488).
- C. Alvarez-Lorenzo and A. Concheiro, Smart Drug Delivery Systems: From Fundamentals to the Clinic, *Chem. Commun.*, 2014, **50**(58), 7743–7765, DOI: [10.1039/c4cc01429d](https://doi.org/10.1039/c4cc01429d).
- J. Franco Machado and T. S. Morais, Are Smart Delivery Systems the Solution to Overcome the Lack of Selectivity of Current Metallodrugs in Cancer Therapy?, *Dalton Trans.*, 2022, **51**(7), 2593–2609, DOI: [10.1039/d1dt04079k](https://doi.org/10.1039/d1dt04079k).
- N. Dixit, Floating Drug Delivery System, *Am. J. PharmTech Res.*, 2011, **10**, 103–122.
- L. Su, Y. Feng, K. Wei, X. Xu, R. Liu and G. Chen, Carbohydrate-Based Macromolecular Biomaterials, *Chem. Rev.*, 2021, **121**(18), 10950–11029, DOI: [10.1021/acs.chemrev.0c01338](https://doi.org/10.1021/acs.chemrev.0c01338).
- J. Brand-Miller, J. McMillan-Price, K. Steinbeck and I. Caterson, Carbohydrates - The Good, the Bad and the Wholegrain, *Asia Pac. J. Clin. Nutr.*, 2008, **17**, 16–19.
- M. Delbianco, P. Bharate, S. Varela-Aramburu and P. H. Seeberger, Carbohydrates in Supramolecular Chemistry, *Chem. Rev.*, 2016, **116**(4), 1693–1752, DOI: [10.1021/acs.chemrev.5b00516](https://doi.org/10.1021/acs.chemrev.5b00516).
- R. Liao, P. Lv, Q. Wang, J. Zheng, B. Feng and B. Yang, Cyclodextrin-Based Biological Stimuli-Responsive Carriers for Smart and Precision Medicine, *Biomater. Sci.*, 2017, **5**(9), 1736–1745, DOI: [10.1039/c7bm00443e](https://doi.org/10.1039/c7bm00443e).
- C. H. Christensen, J. Rass-Hansen, C. C. Marsden, E. Taarning and K. Egeblad, The Renewable Chemicals Industry, *ChemSusChem*, 2008, **1**(4), 283–289, DOI: [10.1002/cssc.200700168](https://doi.org/10.1002/cssc.200700168).
- A. Mittal, Krishna, Aarti, S. Prasad, P. K. Mishra, S. K. Sharma and B. Parshad, Self-Assembly of Carbohydrate-Based Small Amphiphiles and Their Applications in Pathogen Inhibition and Drug Delivery: A Review, *Mater. Adv.*, 2021, **2**(11), 3459–3473, DOI: [10.1039/d0ma00916d](https://doi.org/10.1039/d0ma00916d).
- F. Al Mughairbi, R. Nawaz, F. Khan, A. Hassan, N. Mahmood, H. T. Ahmed, A. Alshamali, S. Ahmed and A. Bashir, Neuroprotective Effects of Bhilawanol and Anacardic Acid during Glutamate-Induced Neurotoxicity, *Saudi Pharm. J.*, 2021, **29**(9), 1043–1049, DOI: [10.1016/j.jsps.2021.07.011](https://doi.org/10.1016/j.jsps.2021.07.011).
- M. A. Indap, R. Y. Ambaye and S. V. Gokhale, Anti Tumour and Pharmacological Effects of the Oil from *Semecarpus Anacardium* Linn. F, *Indian J. Physiol. Pharmacol.*, 1983, **27**(2), 83–91.
- N. S. P. Rao, L. R. Row and R. T. Brown, Phenolic Constituents of *Semecarpus Anacardium*, *Phytochemistry*, 1973, **12**(3), 671–681, DOI: [10.1016/S0031-9422\(00\)84463-5](https://doi.org/10.1016/S0031-9422(00)84463-5).
- A. Thamizhanban, S. Balaji, K. Lalitha, Y. S. Prasad, R. V. Prasad, R. A. Kumar, C. U. Maheswari, V. Sridharan and S. Nagarajan, Glycolipid-Based Oleogels and Organogels: Promising Nanostructured Structuring Agents, *J. Agric. Food Chem.*, 2020, **68**(50), 14896–14906, DOI: [10.1021/acs.jafc.0c02936](https://doi.org/10.1021/acs.jafc.0c02936).
- K. Lalitha, V. Sridharan, C. U. Maheswari, P. K. Vemula and S. Nagarajan, Morphology Transition in Helical Tubules of a Supramolecular Gel Driven by Metal Ions, *Chem. Commun.*, 2017, **53**(9), 1538–1541, DOI: [10.1039/c6cc09120b](https://doi.org/10.1039/c6cc09120b).
- M. I. P. Reis, M. T. Mendes, F. De C. Da Silva and V. F. Ferreira,  $\delta$ -Gluconolactone in Organic Synthesis, *Rev. Virtual Quim.*, 2011, 247–274, DOI: [10.5935/1984-6835.20110032](https://doi.org/10.5935/1984-6835.20110032).
- M. Semalty, A. Semalty, A. Badola, G. P. Joshi and M. S. M. Rawat, *Semecarpus Anacardium* Linn.: A Review, *Pharmacogn. Rev.*, 2010, **4**, 88–94, DOI: [10.4103/0973-7847.65328](https://doi.org/10.4103/0973-7847.65328).
- N. Baccile, C. Seyrig, A. Poirier, S. A. Castro, S. L. K. W. Roelants and S. Abel, Self-assembly, interfacial properties, interactions with macromolecules and molecular modelling and simulation of microbial bio-based amphiphiles (biosurfactants). A tutorial review, *Green Chem.*, 2021, 3842–3944, DOI: [10.1039/d1gc00097g](https://doi.org/10.1039/d1gc00097g).
- P. K. Vemula and G. John, Crops : A Green Approach toward Self-Assembled Soft Materials, *Acc. Chem. Res.*, 2008, **41**(6), 769–782.
- G. John and P. K. Vemula, Design and Development of Soft Nanomaterials from Biobased Amphiphiles, *Soft Matter*, 2006, **2**(11), 909–914, DOI: [10.1039/b609422h](https://doi.org/10.1039/b609422h).
- A. H. Gröschel and A. H. E. Müller, Self-Assembly Concepts for Multicompartment Nanostructures, *Nanoscale*, 2015, 11841–11876, DOI: [10.1039/c5nr02448j](https://doi.org/10.1039/c5nr02448j).
- K. Lalitha, Y. S. Prasad, V. Sridharan, C. U. Maheswari, G. John and S. Nagarajan, A Renewable Resource-Derived Thixotropic Self-Assembled Supramolecular Gel: Magnetic



- Stimuli Responsive and Real-Time Self-Healing Behaviour, *RSC Adv.*, 2015, 5(95), 77589–77594, DOI: [10.1039/c5ra14744a](https://doi.org/10.1039/c5ra14744a).
- 24 A. Roy, K. Manna and S. Pal, Recent Advances in Various Stimuli-Responsive Hydrogels : From Synthetic Designs to Emerging Healthcare Applications, *Mater. Chem. Front.*, 2022, 2338–2385, DOI: [10.1039/d2qm00469k](https://doi.org/10.1039/d2qm00469k).
- 25 S. Zhang, Fabrication of Novel Biomaterials through Molecular Self-Assembly, *Nat. Biotechnol.*, 2003, 21(10), 1171–1178, DOI: [10.1038/nbt874](https://doi.org/10.1038/nbt874).
- 26 P. K. Vemula, J. Li and G. John, Enzyme Catalysis: Tool to Make and Break Amygdalin Hydrogelators from Renewable Resources: A Delivery Model for Hydrophobic Drugs, *J. Am. Chem. Soc.*, 2006, 128(27), 8932–8938, DOI: [10.1021/ja062650u](https://doi.org/10.1021/ja062650u).
- 27 A. Prathap and K. M. Sureshan, Sugar-Based Organogelators for Various Applications, *Langmuir*, 2019, 35, 6005–6014, DOI: [10.1021/acs.langmuir.9b00506](https://doi.org/10.1021/acs.langmuir.9b00506).
- 28 W. Zhang and C. Gao, Morphology Transformation of Self-Assembled Organic Nanomaterials in Aqueous Solution Induced by Stimuli-Triggered Chemical Structure Changes, *J. Mater. Chem. A*, 2017, 5, 16059–16104, DOI: [10.1039/c7ta02038d](https://doi.org/10.1039/c7ta02038d).
- 29 S. Mondal, S. Das and A. K. Nandi, A Review on Recent Advances in Polymer and Peptide Hydrogels, *Soft Matter*, 2020, 16(6), 1404–1454, DOI: [10.1039/c9sm02127b](https://doi.org/10.1039/c9sm02127b).
- 30 A. Thamizhanban, K. Lalitha, G. P. Sarvepalli, C. U. Maheswari, V. Sridharan, J. B. B. Rayappan and S. Nagarajan, Smart Supramolecular Gels of Enolizable Amphiphilic Glycosylfuran, *J. Mater. Chem. B*, 2019, 7(40), 6238–6246, DOI: [10.1039/c9tb01480b](https://doi.org/10.1039/c9tb01480b).
- 31 Y. Siva Prasad, S. Manikandan, K. Lalitha, M. Sandeep, R. Vara Prasad, R. Arun Kumar, C. S. Srinandan, C. Uma Maheswari, V. Sridharan and S. Nagarajan, Supramolecular Gels of Gluconamides Derived from Renewable Resources: Antibacterial and Anti-biofilm Applications, *Nano Sel.*, 2020, 1(5), 510–524, DOI: [10.1002/nano.202000058](https://doi.org/10.1002/nano.202000058).
- 32 L. Faure, S. Nagarajan, H. Hwang, C. L. Montgomery, B. R. Khan, G. John, P. Koulen, E. B. Blancaflor and K. D. Chapman, Synthesis of Phenoxyacyl-Ethanolamides and Their Effects on Fatty Acid Amide Hydrolase Activity, *J. Biol. Chem.*, 2014, 289(13), 9340–9351.
- 33 A. K. Rachamalla, V. P. Rebaka, T. Banoo, R. Pawar, M. Faizan, K. Lalitha and S. Nagarajan, A Facile Synthesis of Amphiphilic N-Glycosyl Naphthalimides and Fabrication of Flexible Semiconductors Using Molecular Self-Assembly, *Green Chem.*, 2022, 24(6), 2451–2463, DOI: [10.1039/d1gc04509a](https://doi.org/10.1039/d1gc04509a).
- 34 H. Satria, K. Kuroda, Y. Tsuge, K. Ninomiya and K. Takahashi, Dimethyl Sulfoxide Enhances Both the Cellulose Dissolution Ability and Biocompatibility of a Carboxylate-Type Liquid Zwitterion, *New J. Chem.*, 2018, 42(16), 13225–13228, DOI: [10.1039/c8nj01912f](https://doi.org/10.1039/c8nj01912f).
- 35 A. Brito, S. Kassem, R. L. Reis, R. V. Ulijn, R. A. Pires and I. Pashkuleva, Carbohydrate Amphiphiles for Supramolecular Biomaterials: Design, Self-Assembly, and Applications, *Chem*, 2021, 2943–2964, DOI: [10.1016/j.chempr.2021.04.011](https://doi.org/10.1016/j.chempr.2021.04.011).
- 36 S. Pakian, F. Radmanesh, H. Sadeghi-Abandansari and M. R. Nabid, Gelatin-Based Injectable Hydrogel/Microgel Composite as a Combinational Dual Drug Delivery System for Local Co-Delivery of Curcumin and 5-Fluorouracil in Synergistic Therapy of Colorectal Cancer, *ACS Appl. Polym. Mater.*, 2022, 4(11), 8238–8252, DOI: [10.1021/acsapm.2c01188](https://doi.org/10.1021/acsapm.2c01188).
- 37 A. Roy, K. Manna and S. Pal, Recent Advances in Various Stimuli-Responsive Hydrogels: From Synthetic Designs to Emerging Healthcare Applications, *Mater. Chem. Front.*, 2022, 6(17), 2338–2385, DOI: [10.1039/d2qm00469k](https://doi.org/10.1039/d2qm00469k).
- 38 F. Khan, M. Atif, M. Haseen, S. Kamal, M. S. Khan, S. Shahid and S. A. A. Nami, Synthesis, Classification and Properties of Hydrogels: Their Applications in Drug Delivery and Agriculture, *J. Mater. Chem. B*, 2022, 10(2), 170–203, DOI: [10.1039/d1tb01345a](https://doi.org/10.1039/d1tb01345a).
- 39 S. S. Das, D. Sharma, B. V. K. Rao, M. K. Arora, J. Ruokolainen, M. Dhanka, H. Singh and K. K. Kesari, Natural Cationic Polymer-Derived Injectable Hydrogels for Targeted Chemotherapy, *Mater. Adv.*, 2023, 4(23), 6064–6091, DOI: [10.1039/d3ma00484h](https://doi.org/10.1039/d3ma00484h).
- 40 Y. S. Prasad, S. Miryala, K. Lalitha, K. Ranjitha, S. Barbhairwala, V. Sridharan, C. U. Maheswari, C. S. Srinandan and S. Nagarajan, Disassembly of Bacterial Biofilms by the Self-Assembled Glycolipids Derived from Renewable Resources, *ACS Appl. Mater. Interfaces*, 2017, 9(46), 40047–40058, DOI: [10.1021/acsami.7b12225](https://doi.org/10.1021/acsami.7b12225).
- 41 K. Lalitha, P. Jenifer, Y. S. Prasad, K. Muthusamy, G. John and S. Nagarajan, A self-assembled  $\pi$ -conjugated system as an anti-proliferative agent in prostate cancer cells and a probe for intra-cellular imaging, *RSC Adv.*, 2014, 4, 48433–48437, DOI: [10.1039/c4ra07710e](https://doi.org/10.1039/c4ra07710e).
- 42 S. J. Hewlings and D. S. Kalman, Curcumin: A Review of Its Effects on Human Health, *Foods*, 2017, 6(10), 1–11, DOI: [10.3390/foods6100092](https://doi.org/10.3390/foods6100092).
- 43 N. Z. Nagy, Z. Varga, J. Mihály, A. Domján, É. Fenyvesi and É. Kiss, Highly Enhanced Curcumin Delivery Applying Association Type Nanostructures of Block Copolymers, Cyclodextrins and Polycyclodextrins, *Polymers*, 2020, 12(9), 2167, DOI: [10.3390/POLYM12092167](https://doi.org/10.3390/POLYM12092167).
- 44 T. C. Ho, C. C. Chang, H. P. Chan, T. W. Chung, C. W. Shu, K. P. Chuang, T. H. Duh, M. H. Yang and Y. C. Tyan, Hydrogels: Properties and Applications in Biomedicine, *Molecules*, 2022, 27(9), 1–29, DOI: [10.3390/molecules27092902](https://doi.org/10.3390/molecules27092902).
- 45 E. Caló and V. V. Khutoryanskiy, Biomedical Applications of Hydrogels: A Review of Patents and Commercial Products, *Eur. Polym. J.*, 2015, 65, 252–267, DOI: [10.1016/j.eurpolymj.2014.11.024](https://doi.org/10.1016/j.eurpolymj.2014.11.024).
- 46 M. Vigata, C. Meinert, D. W. Hutmacher and N. Bock, Hydrogels as Drug Delivery Systems: A Review of Current Characterization and Evaluation Techniques, *Pharmaceutics*, 2020, 12(12), 1–45, DOI: [10.3390/pharmaceutics12121188](https://doi.org/10.3390/pharmaceutics12121188).
- 47 N. P. Pathak, A. Sengupta and S. Yadav, Structure-Gelation Property Relationships of Phenolic Glycosides of Pentose Sugars: PH Dependent Controlled Release of Curcumin, *Mater. Adv.*, 2022, 3, 3906–3914, DOI: [10.1039/d1ma00907a](https://doi.org/10.1039/d1ma00907a).



- 48 M. Huang, B. T. Zhai, Y. Fan, J. Sun, Y. J. Shi, X. F. Zhang, J. B. Zou, J. W. Wang and D. Y. Guo, Targeted Drug Delivery Systems for Curcumin in Breast Cancer Therapy, *Int. J. Nanomed.*, 2023, **18**, 4275–4311, DOI: [10.2147/IJN.S410688](https://doi.org/10.2147/IJN.S410688).
- 49 A. Z. Alkilani, M. T. C. McCrudden and R. F. Donnelly, Transdermal Drug Delivery: Innovative Pharmaceutical Developments Based on Disruption of the Barrier Properties of the Stratum Corneum, *Pharmaceutics*, 2015, **7**(4), 438–470, DOI: [10.3390/pharmaceutics7040438](https://doi.org/10.3390/pharmaceutics7040438).
- 50 H. Ding, P. Tan, S. Fu, X. Tian, H. Zhang, X. Ma, Z. Gu and K. Luo, Preparation and Application of PH-Responsive Drug Delivery Systems, *J. Controlled Release*, 2022, **348**, 206–238, DOI: [10.1016/j.jconrel.2022.05.056](https://doi.org/10.1016/j.jconrel.2022.05.056).
- 51 T. Riss, A. Niles, R. Moravec, N. Karassina and J. Vidugiriene, Cytotoxicity Assays: In Vitro Methods to Measure Dead Cells, *Assay Guidance Manual*, 2019, pp. 1–15.
- 52 X. Du, J. Zhou, J. Shi and B. Xu, Supramolecular Hydrogelators and Hydrogels: From Soft Matter to Molecular Biomaterials, *Chem. Rev.*, 2015, **115**(24), 13165–13307, DOI: [10.1021/acs.chemrev.5b00299](https://doi.org/10.1021/acs.chemrev.5b00299).
- 53 S. A. Holey and R. R. Nayak, Harnessing Glycolipids for Supramolecular Gelation: A Contemporary Review, *ACS Omega*, 2024, **9**(24), 25513–25538, DOI: [10.1021/acsomega.4c00958](https://doi.org/10.1021/acsomega.4c00958).
- 54 Th. J. Snædal, Promiscuous Acyltransferases For Biosurfactant Synthesis, Degree project in Industrial and Environmental Biotechnology. <https://kth.diva-portal.org/smash/record.jsf?pid=diva2%3A1914685>.
- 55 W. Y. Cho, J. F. Ng and W. H. Yap, Sophorolipids — Bio-Based Antimicrobial Formulating Agents, *Molecules*, 2022, **27**(5556), 1–24.
- 56 M. Lourenço, N. Duarte and I. A. C. Ribeiro, Exploring Biosurfactants as Antimicrobial Approaches, *Pharmaceutics*, 2024, **17**(9), 1239, DOI: [10.3390/ph17091239](https://doi.org/10.3390/ph17091239).
- 57 C. Ceresa, L. Fracchia, E. Fedeli, C. Porta and I. M. Banat, Recent Advances in Biomedical, Therapeutic and Pharmaceutical Applications of Microbial Surfactants, *Pharmaceutics*, 2021, **13**(4), 466, DOI: [10.3390/pharmaceutics13040466](https://doi.org/10.3390/pharmaceutics13040466).
- 58 Y. S. Prasad, S. Miryala, K. Lalitha, B. Saritha, C. U. Maheswari, V. Sridharan, C. S. Srinandan and S. Nagarajan, An Injectable Self-Healing Anesthetic Glycolipid-Based Oleogel with Antibiofilm and Diabetic Wound Skin Repair Properties, *Sci. Rep.*, 2020, **10**(1), 1–12, DOI: [10.1038/s41598-020-73708-7](https://doi.org/10.1038/s41598-020-73708-7).
- 59 S. A. Holey, K. P. C. Sekhar, D. K. Swain, S. Bojja and R. R. Nayak, Supramolecular Glycolipid-Based Hydro-/Organogels with Enzymatic Bioactive Release Ability by Tuning the Chain Length and Headgroup Size, *ACS Biomater. Sci. Eng.*, 2022, **8**(3), 1103–1114, DOI: [10.1021/acsbomaterials.1c01510](https://doi.org/10.1021/acsbomaterials.1c01510).
- 60 P. Jain and H. P. Sharma, A Potential Ethnomedicinal Plant *Semecarpus Anacardium* Linn. – A Review, *Int. J. Res. Pharm. Chem.*, 2013, **3**(3), 564–572.
- 61 T. K. Mohanta, J. K. Patra, S. K. Rath, D. K. Pal and H. N. Thatoi, Evaluation of Antimicrobial Activity and Phytochemical Screening of Oils and Nuts of *Semecarpus Anacardium* L., *Sci. Res. Essays*, 2007, **2**, 486–490.
- 62 P. Bandigari and A. Dongamanti, Purification, Extraction of *Semecarpus Anacardium* by Traditional Method and Evaluation of Antibacterial Activity, *J. Med. Pharm. Allied Sci.*, 2021, **10**(2320), 3633–3635, DOI: [10.22270/jmpas.V10I5.1430](https://doi.org/10.22270/jmpas.V10I5.1430).
- 63 J. N. Weiser, D. M. Ferreira and J. C. Paton, *Streptococcus pneumoniae*: transmission, colonization and invasion, *Nat. Rev. Microbiol.*, 2018, **16**, 355–367, DOI: [10.1038/s41579-018-0001-8](https://doi.org/10.1038/s41579-018-0001-8). **Streptococcus**.
- 64 T. Sawada, M. Katayama, S. Takatani and Y. Ohiro, Early Detection of Drug-Resistant *Streptococcus Pneumoniae* and *Haemophilus Influenzae* by Quantitative Flow Cytometry, *Sci. Rep.*, 2021, **11**(1), 1–8, DOI: [10.1038/s41598-021-82186-4](https://doi.org/10.1038/s41598-021-82186-4).
- 65 A. M. Barceló, I. C. Cortina, A. I. A. Rodríguez and C. R. Ballesteros, Climatología Del Balneario de Villavieja, *An. R. Acad. Nac. Farm.*, 2016, **82**(5), 108–126.
- 66 S. Fu and X. Yang, Recent advances in natural small molecules as drug delivery systems, *J. Mater. Chem. B*, 2023, **11**, 4584–4599, DOI: [10.1039/d3tb00070b](https://doi.org/10.1039/d3tb00070b).
- 67 Z. Breijyeh, B. Jubeh and R. Karaman, Resistance of Gram-Negative Bacteria to Current Antibacterial Agents and Approaches to Resolve It, *Molecules*, 2020, **25**(6), 1340.
- 68 P. L. Wantuch and F. Y. Avci, Current Status and Future Directions of Invasive Pneumococcal Diseases and Prophylactic Approaches to Control Them, *Hum. Vaccines Immunother.*, 2018, **14**, 2303–2309, DOI: [10.1080/21645515.2018.1470726](https://doi.org/10.1080/21645515.2018.1470726).
- 69 Y. S. Choi, K. H. Kim, D. G. Kim, H. J. Kim, S. H. Cha and J. C. Lee, Synthesis and Characterization of Self-Cross-Linkable and Bactericidal Methacrylate Polymers Having Renewable Cardanol Moieties for Surface Coating Applications, *RSC Adv.*, 2014, **40**(78), 41195–41203, DOI: [10.1039/c4ra06223j](https://doi.org/10.1039/c4ra06223j).
- 70 Y. S. Choi, N. K. Kim, H. Kang, H. K. Jang, M. Noh, J. Kim, D. J. Shon, B. S. Kim and J. C. Lee, Antibacterial and Biocompatible ABA-Triblock Copolymers Containing Perfluoropolyether and Plant-Based Cardanol for Versatile Coating Applications, *RSC Adv.*, 2017, **7**(60), 38091–38099, DOI: [10.1039/c7ra07689d](https://doi.org/10.1039/c7ra07689d).

